Quasiparticle band structure of $SrTiO_3$ and $BaTiO_3$: A combined LDA + U and G^0W^0 approach

Gabriel Lopez-Candales,[1] Zhao Tang,[1] Weiyi Xia,[1] Fanhao Jia,[1,2] and Peihong Zhang[1,*]

[1]*Department of Physics, University at Buffalo, State University of New York, Buffalo, New York 14260, USA*

[2]*Physics Department, International Centre of Quantum and Molecular Structures, Shanghai University, Shanghai 200444, China*

(Received 6 October 2020; revised 19 December 2020; accepted 4 January 2021; published 19 January 2021)

We present the quasiparticle band structures of prototypical oxide perovskites $SrTiO_3$ and $BaTiO_3$, two seemingly simple oxides for which accurate calculations of the electronic structure have been met with significant (and somewhat unexpected) challenges. Previous G^0W^0 calculations predicted a band gap ranging from 3.36 to 3.82 eV for $SrTiO_3$, with a majority of the studies giving a band gap around 3.7 $\sim$ 3.8 eV, to be compared with the experimental value of 3.25 eV. A similar discrepancy between theory and experiment is also observed for $BaTiO_3$. We show that the G^0W^0 approach can predict reasonably accurate band gaps of $SrTiO_3$ and $BaTiO_3$, provided that the calculations are carried out on top of the local density approximation (LDA) plus U (LDA + U) solutions and are fully converged. The deficiency of the LDA in describing the localized 3d states, although not particularly critical in this case, still results in a poor mean-field starting point for subsequent many-body perturbation calculations. G^0W^0 calculations starting from the LDA + U solutions, on the other hand, give significantly improved results for both systems. Our work demonstrates the accuracy and applicability of the combined G^0W^0 and LDA + U approach in calculating the quasiparticle band structures for materials involving localized 3d states, not only for systems with fully occupied 3d semicore states as has been shown before, but also for systems in which the 3d states are nominally unoccupied.

DOI: 10.1103/PhysRevB.103.035128

I. INTRODUCTION

Many-body perturbation theory within the GW approximation [1–4] has been established as one of the most successful first-principles methods for calculating the quasiparticle properties of solids. Most first-principles GW calculations are carried out using the G^0W^0 (also known as one-shot GW) approach in which the electron self-energy is treated as a first-order correction to the Kohn-Sham eigenvalue, typically calculated within the local density approximation (LDA) [5–7] or the generalized gradient approximation (GGA) [8,9], without further iterations. The G^0W^0 approach, with its relative simplicity and computational efficiency, has been applied to the study of a wide range of weakly to moderately correlated materials with great success. However, there are notable exceptions, i.e., the G^0W^0 approach does not seem to be able to give satisfactory results for a number of material systems that are not normally considered strongly correlated, raising questions about the accuracy of the G^0W^0 approach. Strontium titanate ($SrTiO_3$) and barium titanate ($BaTiO_3$) are two such systems that have received much research attention.

$SrTiO_3$ and $BaTiO_3$ belong to an interesting class of titanium-based perovskites which possess a number of intriguing and useful properties. These materials have attracted continuous research interest for both practical applications and understanding fundamental quantum physics. $SrTiO_3$ has found important applications in photocatalysis [10–13], solid fuel cells [14], and other energy-related applications [15]. Perhaps more significant is the discovery of a high-density and high-mobility two-dimensional electron gas formed at the interface between $SrTiO_3$ and $LaAlO_3$ [16], which has been shown to give rise to a number of exotic properties such as superconductivity [17] and ferromagnetism [18] and paves the way for future oxide-based electronic devices [19,20]. At low temperatures, $SrTiO_3$ is also a fascinating quantum paraelectric [21] in which quantum fluctuations stabilize the paraelectric phase, suppressing the onset of ferroelectric order. $BaTiO_3$ is one of the most investigated ferroelectric materials. Beyond its common applications in capacitors and sensors, $BaTiO_3$ also displays a range of interesting properties that may be closely related to its ferroelectricity such as bulk photovoltaic effects [22–25] and positive temperature coefficient of resistivity [26,27].

The basic structural and electronic properties of these titanate perovskites have been well understood. Above the phase transition temperature ($T_C \approx 105$ K), $SrTiO_3$ is a classical paraelectric material assuming a centrosymmetric simple cubic structure with an indirect gap ($\Gamma \rightarrow$ R) of about 3.20 $\sim$ 3.25 eV and a direct gap at the Γ point of 3.75 eV [28–32]. $BaTiO_3$, on the other hand, is a ferroelectric material assuming a tetragonal structure at room temperature with an indirect band gap ($\Gamma \rightarrow$ A) of about 3.15 $\sim$ 3.20 eV [28,33], and a direct gap of about 3.6 eV [28,29]. On the theory side, straightforward G^0W^0 calculations on top of the LDA or GGA Kohn-Sham solution give an indirect gap of $SrTiO_3$ ranging from 3.36 to 3.82 [34–40]. It is noteworthy that most calculations give a band gap toward the higher end of the range, i.e., around 3.7 $\sim$ 3.8 eV, which is significantly larger than the experimental value. In addition, such a wide spread of

*pzhang3@buffalo.edu

results that are calculated at the (supposedly) same level of theory is puzzling and disturbing. As for $BaTiO_3$, a previous G^0W^0 calculation gives an indirect gap of 3.90 eV [41] for the room-temperature tetragonal phase, which is also much larger than the experimental value of 3.15 $\sim$ 3.20 eV [28,33].

In fact, there is another class of seemingly simple semiconductors (e.g., ZnO, CuCl, and CuBr, to name a few) for which G^0W^0 calculations (starting from the LDA or GGA solutions) also fail to give reasonable results. However, the significant overestimation of the quasiparticle band gap for titanates is quite the opposite when compared to these systems. For example, straightforward G^0W^0 calculations significantly underestimate the band gaps of for ZnO and CuCl [42–45]. For these systems it has been shown that the inaccurate treatment of the localized 3*d* states using the local or semilocal functionals can have profound effects on calculated quasiparticle properties. The LDA functional under-binds (and delocalizes) the 3*d* states, leading to an inaccurate description of the chemical hybridization effects and thus poor zeroth-order solutions for subsequent many-body perturbation calculations. In addition, *GW* calculations for these systems are notoriously difficult to converge, an issue that is closely related to the involvement of localized *d* states.

It is now well established that the LDA + *U* [46,47] method gives an improved description of the localized 3*d* states in solids. Thus the LDA + *U* mean-field solution may provide a better starting point for subsequent many-body perturbation calculations. Indeed, if the G^0W^0 calculations are carried out on top of the LDA + *U* mean-field solutions, significantly improved results can be achieved for ZnO and CuCl [42,44] and other systems [48,49]. Even though the Ti 3*d* states are nominally unoccupied in titanate perovskites, it is likely that the deficiency of the LDA functional in describing the localized 3*d* states will still have significant effects on the *GW* results. In this work we show that the overestimation of the quasiparticle band gaps of titanate perovskites can largely be resolved if the *GW* calculations are carried out using the LDA + *U* solutions as a starting point, provided that the calculations are properly converged. The calculated indirect band gaps of $SrTiO_3$ and $BaTiO_3$ are 3.38 and 3.25 eV, respectively, which agree well with the experimental results of 3.25 and 3.15 eV and are well within the typical accuracy of the G^0W^0 approach for semiconductors. The convergence issue of the *GW* calculations of these systems will also be discussed in detail.

II. COMPUTATIONAL DETAILS

The pseudopotential plane-wave-based density functional theory (DFT) calculations are carried out using a local version of the PARATEC package [50]. We use the Troullier-Martins norm-conserving pseudopotential [51]. Semicore states, namely, Ti 3*s* and 3*p*, Sr 4*s* and 4*p*, and Ba 5*s* and 5*p*, are included as valence electrons in the calculations. In order to describe accurately the fairly localized semicore states, we used a high plane-wave cutoff energy of 175 Ry for both systems. The Brillouin zone integration is carried out using a $6 \times 6 \times 6$ uniform *k* grid. The electronic structures are calculated using the structures of the room-temperature phases, namely, cubic phase for $SrTiO_3$ and tetragonal phase for $BaTiO_3$, as shown in Fig. 1. Room-temperature experimental structural parameters [52,53] are used in DFT and *GW* calculations.

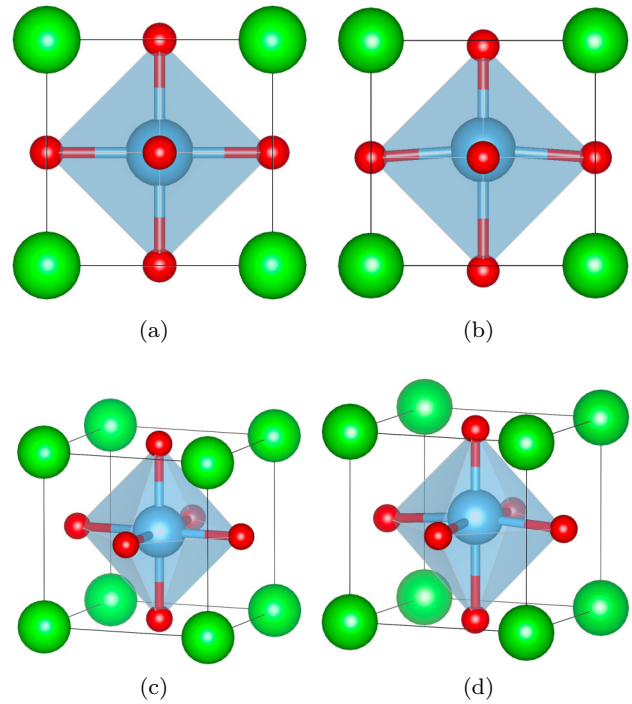

FIG. 1. Crystal structures of room-temperature titanate perovskites: (a, c) cubic-phase $SrTiO_3$, (b, d) tetragonal-phase $BaTiO_3$.

The *GW* quasiparticle calculations are carried out using a local version of the BERKELEY GW package [54]. The recently developed acceleration technique [55] is employed to evaluate the summations over a large number of conduction bands. Using this method we are able to include *all* conduction bands in our *GW* calculations at a fraction of the computational cost compared with the conventional band-by-band summation approach. The Hybertsen-Louie generalized plasmon-pole (HL-GPP) model [3] is used to extend the static dielectric function to finite frequencies.

In the LDA + *U* method [46,47] the energy functional consists of three contributions:

$$E^{\mathrm{LDA}+U} = E^{\mathrm{LDA}}[\rho(\mathbf{r})] + E^{U}[\mathbf{n}] + E^{\mathrm{dc}}[\mathbf{n}], \qquad (1)$$

where $E^{\mathrm{LDA}}[\rho(\mathbf{r})]$ is the usual LDA functional of charge density ρ, $E^{U}[\mathbf{n}]$ is the on-site Coulomb interaction among (identified) localized electrons with $\mathbf{n}$ being the orbital occupation density matrix, and $E^{\mathrm{dc}}[\mathbf{n}]$ is the double counting term. In this work, the on-site Coulomb *U* potential is applied to the Ti 3*d* orbitals. We use a moderate Coulomb *U* of 4.5 eV and an exchange *J* of 0.5 eV for both systems, resulting in an effective $U^{\mathrm{eff}} = U - J$ of 4.0 eV. For *GW* calculations starting from the LDA + *U* solution (which will be referred to as *GW* /LDA + *U* hereafter), the self-energy correction $\delta\Sigma$ to the Kohn-Sham eigenvalues becomes

$$\delta\Sigma^{GW} = \Sigma^{GW} - V_{\mathrm{xc}}^{\mathrm{LDA}+U} = \Sigma^{GW} - \left(V_{\mathrm{xc}}^{\mathrm{LDA}} + \delta\mathbf{V}^{U}\right), \qquad (2)$$

where $V_{\mathrm{xc}}^{\mathrm{LDA}}$ is the LDA exchange-correlation (xc) potential, and $\delta\mathbf{V}^{U}$ is the orbital-dependent xc potential (matrix)

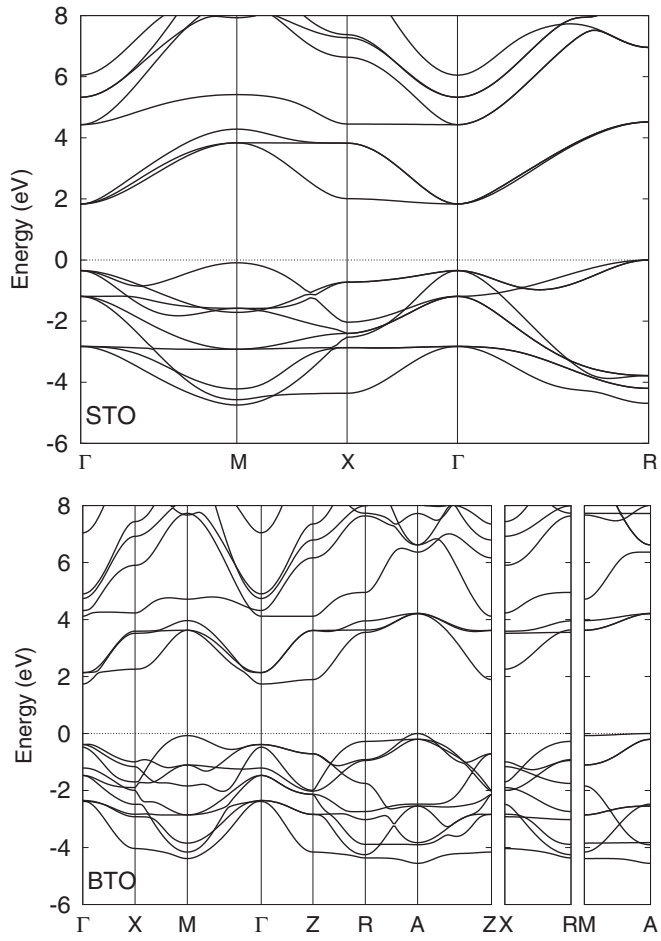

FIG. 2. LDA band structures of cubic $SrTiO_3$ (top) and the tetragonal $BaTiO_3$ (bottom).

arising from the on-site Coulomb interaction in the LDA + U functional. Details of the implementation of the LDA + U method in pseudopotential plane-wave calculations and the GW/LDA + U method can be found in our previous work [56,57].

III. RESULTS AND DISCUSSION

A. DFT and *GW* band structures of $SrTiO_3$ and $BaTiO_3$

The electronic band structures of $SrTiO_3$ and $BaTiO_3$ calculated within DFT are now well understood. Here we summarize a few main features for the completeness of our discussion. Figure 2 shows the LDA band structures of the cubic-phase $SrTiO_3$ and the tetragonal phase $BaTiO_3$. The lower conduction bands are mainly coming from localized Ti 3d states while the upper valence bands are of O 3p character. The direct (at Γ) and indirect (Γ → R) band gaps of $SrTiO_3$ calculated within the LDA are 2.15 and 1.79 eV, respectively; those for $BaTiO_3$ are 2.14 (at Γ) and 1.75 eV (Γ → A). Unlike in the cases of ZnO or CuCl, for which the LDA severely underestimates the band gaps [42,44], the LDA results for $SrTiO_3$ and $BaTiO_3$, although significantly smaller than the experimental values, appear to be within the norm.

TABLE I. Direct and indirect band gaps for $SrTiO_3$ and $BaTiO_3$ calculated at different levels (LDA, LDA + U, GW/LDA, and GW/LDA + U), where all values are given in electronvolts.

	E_g^{dir}					E_g^{ind}				
	$U=0$		$U=4$		Exp	$U=0$		$U=4$		Exp
	DFT	GW	DFT	GW		DFT	GW	DFT	GW	
STO	2.15	4.15	2.62	3.83	3.75	1.79	3.75	2.21	3.38	3.25
BTO	2.14	4.02	2.54	3.69	3.60	1.75	3.62	2.14	3.23	3.15

Our GW/LDA results are consistent with previous work in that the calculated band gaps (both direct and indirect gaps) are about 0.4 ∼ 0.5 eV larger than the experimental values, as shown in Table I. For example, the calculated direct and indirect gaps of $SrTiO_3$ are 4.15 and 3.75 eV, respectively, to be compared with experimental values of 3.75 and 3.25 eV. We have carefully checked the convergence of our calculations with respect to various truncation parameters as will be discussed later. Therefore even though LDA results for $SrTiO_3$ and $BaTiO_3$ appear to be acceptable, it is likely that the deficiency of the LDA in the description of the localized d states will still have significant effects, albeit to a lesser degree since the Ti 3d are not as localized as the Zn or Cu 3d states. The band structures calculated using the LDA + U method are qualitatively similar to those shown in Fig. 2, so we will not show here. However, applying a moderate on-site Coulomb U ($U^{\rm eff} = 4.0$ eV) noticeably improves the calculated band gap (by about 0.5 eV for both systems) as shown in Table I.

It would be interesting to see if GW calculations on top of the LDA + U solution can lead to a better prediction of the quasiparticle band gaps for these systems. In fact, one may expect the opposite since GW/LDA calculations already overestimate the band gaps; assuming similar quasiparticle corrections, the GW/LDA + U approach may predict even larger band gaps. Therefore it is somewhat surprising that our GW/LDA + U calculations actually give significantly smaller quasiparticle band gaps, both the direct gaps at Γ and the indirect gaps, for both systems as shown in Table I. The calculated band gaps are now well within the typical accuracy of the G^0W^0 method, about 0.08 ∼ 0.13 eV larger than the experimental results, as opposed to the GW/LDA results which are 0.4 to 0.5 eV larger. Figure 3 shows the quasiparticle band structures of $SrTiO_3$ (top) and $BaTiO_3$ (bottom) calculated using the GW/LDA + U approach. In addition to the enhanced band gaps (which now agree rather well with experiment), the valence bandwidths are also enhanced (by 0.49 eV for $SrTiO_3$ and 0.45 eV for $BaTiO_3$) compared with the corresponding LDA values.

B. Understanding the effects of the Coulomb U on the *GW* results

It should be pointed out that the improvement in the calculated Kohn-Sham band gap within the LDA + U method is not particularly important for subsequent GW calculations since the on-site Coulomb potential contribution to the quasiparticle energy is subtracted from the self-energy correction in the GW calculation [see Eq. (2)]. The more consequential

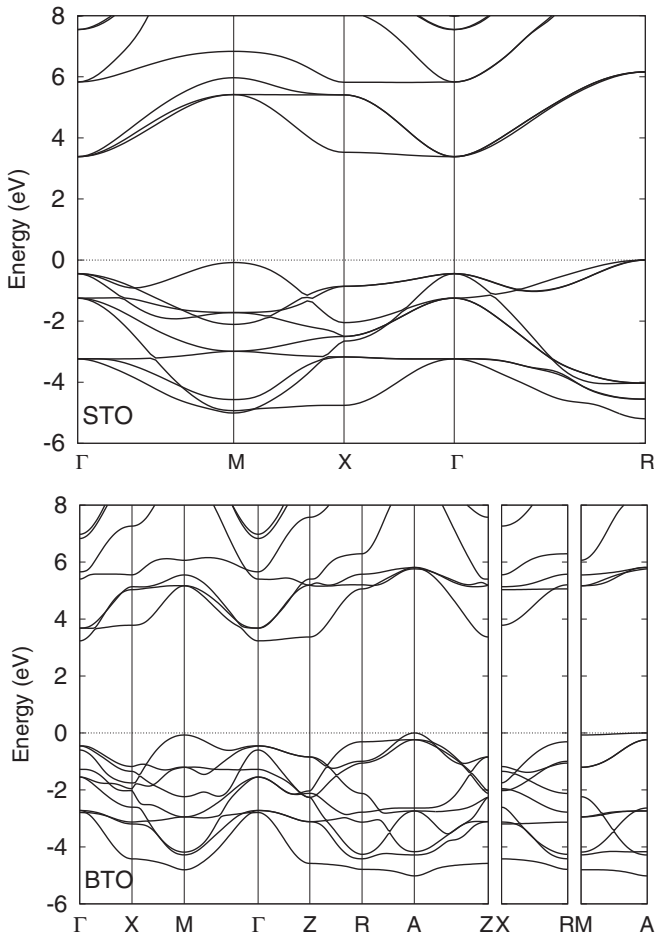

FIG. 3. *GW* band structures of cubic $SrTiO_3$ (top) and tetragonal $BaTiO_3$ (bottom).

effect of the LDA + U functional is the subtle changes to the *pd* hybridization and the Kohn-Sham wave functions. Although the Ti 3*d* states are nominally unoccupied in these systems, charge analyses reveal small but not negligible *d* occupations through the hybridization with oxygen *p* states. Table II shows the calculated *d* occupations by projecting the occupied states onto the atomic Ti *d* states. The LDA + U functional gives slightly smaller *d* occupations compared to the LDA, presumably a result of the reduced *pd* hybridization. These delicate changes to Kohn-Sham wave functions within the LDA + U likely provide an improved zeroth-order solution for subsequent *GW* calculations.

A more detailed investigation of the different contributions to the self-energy may provide additional insight into the

TABLE II. Calculated occupations of Ti 3*d* states and high-frequency dielectric constants within the LDA and the LDA + U methods.

	$SrTiO_3$			$BaTiO_3$		
	LDA	LDA + U	Exp.	LDA	LDA + U	Exp.
d occupation	1.71	1.57		1.80	1.66	
ϵ_∞	6.22	5.53	5.30	6.00	5.53	5.30

TABLE III. Various contributions to the quasiparticle energies of the VBM and CBM states of $SrTiO_3$: Comparison between the *GW*/LDA and *GW*/LDA + U methods.

VBM (R)	Σ_{SX}	Σ_{CH}	Σ	V_{xc}	$\delta\Sigma$
GW/LDA	−8.229	−13.739	−21.968	−20.045	−1.923
GW/LDA+U	−8.555	−13.528	−22.083	−20.050	−2.033
GW/LDA (sc)	−8.409	−13.588	−21.997	−20.045	−1.952
CBM (Γ)	Σ_{SX}	Σ_{CH}	Σ	V_{xc}	$\delta\Sigma$
GW/LDA	−3.908	−14.713	−18.621	−19.022	+0.401
GW/LDA+U	−3.909	−14.357	−18.266	−17.658	−0.608
GW/LDA (sc)	−3.914	−14.651	−18.565	−19.022	+0.457

effects of the on-site Coulomb U on the *GW* results. The electron self-energy can be decomposed into screened exchange (Σ_{SX}) and Coulomb-hole (Σ_{CH}) terms as shown in Table III, using the results for $SrTiO_3$ as an example. Note that the self-energy results shown in Table III are calculated at the DFT Kohm-Sham eigenvalues, i.e., $\Sigma(E = \epsilon_{n\mathbf{k}}^{DFT})$. Although the VBM (valence band maximum) state (at the R point) does not have the Ti 3*d* wave-function components, both the Σ_{SX} and Σ_{CH} terms for the VBM state are still noticeably affected by the application of the Coulomb U in the calculations. The calculated Σ_{SX} is enhanced from −8.229 eV (*GW*/LDA) to −8.555 eV (*GW*/LDA + U). On the other hand, Σ_{CH} is reduced from −13.739 eV to −13.528 eV. These results can be largely ascribed to the reduced dielectric screening (as a result of enhanced DFT band gap) in the *GW*/LDA + U calculations, as shown in Table II. For example, the calculated (high-frequency) dielectric constant (ϵ_∞) of $SrTiO_3$ is 5.53 within the LDA + U method, to be compared with the LDA result of 6.22 and the experimental value of 5.30 [28].

In fact, if we simply apply a scissors shift (sc) to the LDA band gap to match that of the LDA + U one, we also obtained an enhanced Σ_{SX} and reduced Σ_{CH} for the VBM state as shown in Table III [the *GW*/LDA (sc) row]. Interestingly, the changes to the Σ_{SX} and Σ_{CH} of the VBM state in the *GW*/LDA (sc) calculations largely cancel out, resulting in an overall self-energy that is practically the same as that in the *GW*/LDA calculation without applying a scissors shift. The differences between the *GW*/LDA and *GW*/LDA + U results for the overall self-energy for the VBM state is also rather small (about 0.1 eV), as shown in Table III. Therefore the bulk of the difference in the calculated quasiparticle gap within the *GW*/LDA + U approach (compared with the *GW*/LDA approach) comes from the CBM (conduction band minimum) state, more specifically, the Σ_{CH} and the mean field V_{xc}, as shown in the lower panel of Table III. Whereas the *GW*/LDA calculations give a positive quasiparticle correction $\delta\Sigma$ to the CBM state, this correction is negative within the *GW*/LDA + U approach. This explains the smaller band gap predicted by the *GW*/LDA + U method. The effects of U on Σ_{SX} for the CBM state are negligible, which is somewhat surprising. We believe this is a result of the canceling effects from the reduced dielectric screening and the slight modification to wave function of the CBM state: the reduced dielectric screening tends to enhance Σ_{SX}, whereas the *pd* hybridization of the CBM state tends to decrease Σ_{SX}.

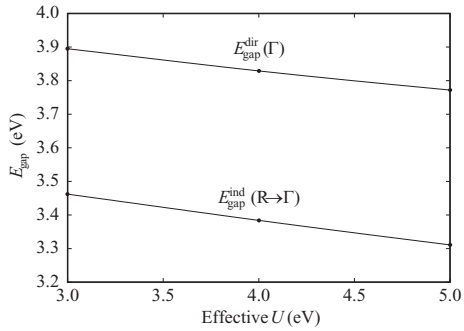

FIG. 4. Calculated indirect and direct *GW* band gaps of $SrTiO_3$ as a function of the effective Coulomb U.

C. Choice of the screened Coulomb U and the sensitivity of the calculated results on U

The idea of introducing a screened onsite Coulomb U for localized electrons in solid-state DFT calculations, although well justified conceptually, does not provide a unique or unambiguous way for evaluating this parameter in practical calculations. Conceptually, the screened Coulomb U for localized electrons in solids can be evaluated:

$$U_{ij} = \int d\mathbf{r}d\mathbf{r}'|\phi_i(\mathbf{r})|^2 W(\mathbf{r},\mathbf{r}')|\phi_j(\mathbf{r}')|^2, \tag{3}$$

where $\phi_i(\mathbf{r})$ are properly defined localized orbitals and $W(\mathbf{r},\mathbf{r}')$ is the screened Coulomb interaction, which is related to the inverse dielectric function ϵ^{-1} via

$$W(\mathbf{r},\mathbf{r}') = \int d\mathbf{r}''\epsilon^{-1}(\mathbf{r},\mathbf{r}'')v(\mathbf{r}'',\mathbf{r}'). \tag{4}$$

There is, however, no unique definition for *localized* states in solids. Often atomiclike orbitals or properly constructed Wannier orbitals are used in practical calculations, leaving room for ambiguity and uncertainty. In addition, it was pointed out that the intrachannel screening (in this case, the *d-d* screening) should be excluded in the calculation of the dielectric function [58–62], resulting in the so-called constrained random-phase approximation (cRPA) method for calculating the screened Coulomb interaction of localized electrons in solids. Again, there is no unique way for projecting out the intrachannel screening. As a result, there is a significant uncertainty in the estimation of this parameter, and it is not unusual that the U parameter for the same system calculated by different groups differ by ± 1 eV or more.

In this work we use a U_{eff} of 4.0 eV for both systems. In fact, we have carried out calculations of the U parameter for $SrTiO_3$ using the cRPA approach that we have developed [61,62] in the past. The calculated bare Coulomb U is 18.5 eV and that for the screened U is about 4.03 eV, suggesting an effective dielectric constant within the cRPA of about 4.6. Compared with the RPA value of the dielectric constant of 5.53 shown in Table II, the removal of the intrachannel (*d-d* channel) screening results in a slight reduction of the dielectric screening. As discussed earlier, these values are not to be taken exactly. Therefore it is prudent to examine the sensitivity of the *GW* results on the choice of U. Figure 4 shows the dependence of the calculated direct and indirect *GW* band gap of $SrTiO_3$ on the Coulomb U parameter. The change in the *GW* band gap is approximately 10% of the change in the U value. If we took $U_{\text{eff}} = 4.0 \pm 0.5$ eV, the calculated indirect gap of $SrTiO_3$ would be 3.38 ± 0.05 eV, which is well within the accuracy of the *GW* method.

D. Convergence behavior of the *GW* results for $SrTiO_3$ and $BaTiO_3$

We now discuss the convergence issues in *GW* calculations using conventional approaches, i.e., *GW* implementations that involve explicit summations over conduction bands. The convergence issue in *GW* calculations has been widely recognized but sometimes received less attention. We will restrict our discussion to the pseudopotential plane-wave-based *GW* calculations using the HL-GPP model since other *GW* implementations (e.g., all-electron or local-basis-based *GW* methods) as well as calculations using different GPP models [63] or without the use of a GPP model may have different convergence behaviors. Conventional *GW* calculations involve two computationally expensive summations [3,42]. The calculation of the dielectric function and the Coulomb-hole (COH) part of the self-energy both require a summation over unoccupied states. For example, the electron polarizability χ^0 (which is related to the dielectric function ϵ via $\epsilon = 1 - V_c\chi^0$, with V_c being the Fourier transform of the bare Coulomb potential) is constructed using the Kohn-Sham eigenstates:

$$\chi^0_{\mathbf{G},\mathbf{G}'}(\mathbf{q},\omega) = \sum_{nn'\mathbf{k}} M_{nn'}(\mathbf{k},\mathbf{q},\mathbf{G})M^*_{nn'}(\mathbf{k},\mathbf{q},\mathbf{G}') \times \left(\frac{f_{n\mathbf{k}} - f_{n'\mathbf{k}+\mathbf{q}}}{\omega + \epsilon_{n\mathbf{k}} - \epsilon_{n'\mathbf{k}+\mathbf{q}} + i\delta}\right), \tag{5}$$

where $M_{nn'}(\mathbf{k},\mathbf{q},\mathbf{G}) = \langle n,\mathbf{k}+\mathbf{q}|e^{i(\mathbf{q}+\mathbf{G})r}|n',\mathbf{k}\rangle$, $f_{n\mathbf{k}}$ is the occupation function of state $|n,\mathbf{k}\rangle$ with eigenvalue $\epsilon_{n\mathbf{k}}$, and n and n' are the band indices. The summation should in principle include *all* conduction bands. In practical calculations, especially for *GW* calculations for complex (large) systems and/or systems involving localized states, one is often forced to only include a small fraction of the total number of conduction bands due to computational constraints, without having *a priori* knowledge of if the results are properly converged or not. One also has to impose a truncation to the dielectric matrix, discarding matrix elements with $\mathbf{G},\mathbf{G}'$ greater than a certain cutoff value $|\mathbf{G}_{\max}|^2 < E^{\epsilon}_{\text{cut}}$. Often $E^{\epsilon}_{\text{cut}}$ is set to a much smaller value than the plane-wave cutoff, since one expects that high-momentum-transfer dielectric screening is not effective. However, for systems involving substantially localized electrons, this truncation parameter must also be carefully checked.

For simple *sp* semiconductors (e.g., Si, Ge, and GaAs, to name a few), *GW* results usually converge quickly with respect to the above-mentioned truncation parameters (i.e., the number of conduction bands N_c and $E^{\epsilon}_{\text{cut}}$). *GW* calculations for more complex materials involving localized *d* states and/or systems with a large unit cell, however, are significantly more challenging. For these systems, *GW* results may converge extremely slowly, requiring a very large number of bands and a high cutoff energy for the dielectric matrix [42,44,55] to achieve properly converged results. In the following discussion, we will set the number of conduction bands used

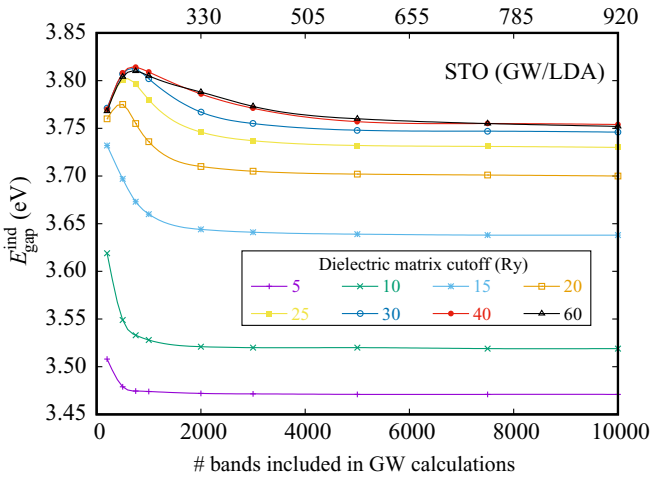

FIG. 5. Convergence behavior of the calculated indirect band gaps of $SrTiO_3$ using the *GW*/LDA approach, illustrating how the choice of truncation parameters can affect the result.

in the dielectric matrix calculations the same as that in the self-energy calculations. We will only discuss the convergence behavior of the *GW*/LDA results for $SrTiO_3$ since the *GW*/LDA + *U* results or the results for $BaTiO_3$ have very similar convergence behaviors. Although the convergence issue is not particularly critical for these two systems, underconverged calculations can still lead to substantially different results.

Figure 5 shows the calculated indirect band gap of $SrTiO_3$ using the *GW*/LDA approach, illustrating how the choice of truncation parameters can affect the result. It is clear that a high-kinetic-energy cutoff ($\sim$ 40 Ry) for the dielectric matrix as well as a large number (>5000, or over 1000 per atom) of conduction bands are needed to properly converge the result. Our work benefits from a recently developed accelerated method [55] in which the band-by-band summation is replaced by an integration in the energy space for high-energy conduction states. With this method we can now carry out converged *GW* calculations (by including *all* conduction states) at a fraction of the computational cost compared with the conventional approach. In Fig. 5, the lower horizontal axis shows the number of bands in conventional *GW* calculations, whereas the upper horizontal axis shows the number of integration points used in our method [55], which represents a speedup factor of over 10 in this case. The calculated band gap ranges from 3.47 to 3.82 eV, depending on cutoff of the dielectric matrix and the number of conduction bands included in the calculation. Interestingly, the spread of the calculated band gap shown in Fig. 5 is also consistent with the reported G^0W^0 results [34–40] for $SrTiO_3$.

In fact, these two parameters (i.e., the cutoff energy for the dielectric matrix and the number of conduction bands included in the calculation) are inter-related. If a small cutoff for the dielectric matrix is used, contributions to the COH self-energy from high-energy conduction states are essentially discarded, as can be seen from Fig. 5. The results calculated using small dielectric matrix cutoffs (e.g., 5 or 10 Ry) show a false convergence behavior with respect to the number of bands included in the calculations. A small cutoff for the dielectric matrix also leads to an underestimation of the screened exchange energy arising from the high-**G** components of the dielectric screening.

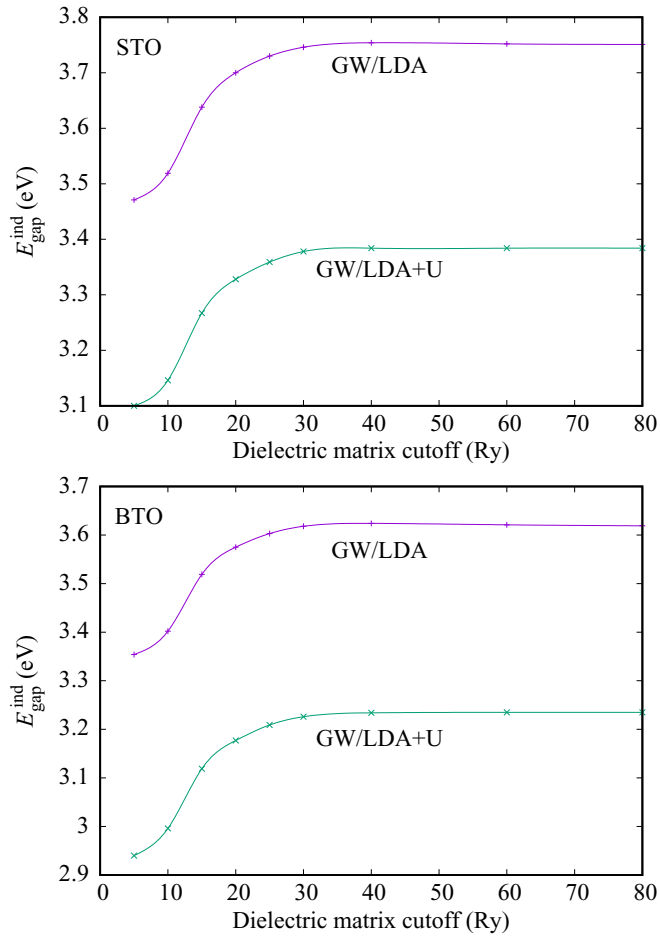

FIG. 6. Calculated indirect band gaps of $SrTiO_3$ (top) and $BaTiO_3$ (bottom) as a function of the cutoff energy of the dielectric matrix using both the *GW*/LDA and *GW*/LDA + *U* approaches.

Figure 6 summarizes the calculated indirect band gap of $SrTiO_3$ and $BaTiO_3$ as a function of the cutoff energy of the dielectric matrix using both *GW*/LDA and *GW*/LDA + *U* approaches. All results presented in Fig. 6 are fully converged with respect to the number of conduction bands included in the calculations. Using the LDA + *U* (as opposed to the LDA) solution as a starting point for subsequent G^0W^0 calculations reduces the calculated band gap by about 0.4 eV with a moderate on-site Coulomb *U* ($U^{\text{eff}} = U - J = 4.0$ eV) for both systems, bringing the calculated results more in line with experimental results and within the typical accuracy of the *GW* method as we have discussed in the previous section.

E. Discussion

Although it is now well established that G^0W^0 calculations on top of the LDA or GGA solution can predict reasonably well quasiparticle band gaps for the most simple (i.e., not strongly correlated) *sp* semiconductor, there are notable exceptions. These systems often involve localized semicore 3*d* states, with ZnO probably being the most discussed and contentious example [42,43,63–66]. Material systems involv-

ing unoccupied 3*d* states such as those discussed in this work have also started to gain attention. The seeming discrepancy between theory and experiment for these systems has raised the question of the accuracy and applicability of the conventional *GW* approach. This issue is well justified and certainly deserves further investigation. It is possible that other physics/interaction (beyond what is considered in the conventional *GW* approach) may need to be included to fully resolve this issue. Recently, Bhandari *et al.* [40] carried out quasiparticle self-consistent *GW* calculations for $SrTiO_3$. The calculated band gaps are found to be much larger than the experimental values, 4.83 eV for the direct gap at Γ and 4.34 eV for the indirect gap, to be compared with experimental values of 3.25 and 3.75 eV, respectively, representing an overestimation of over 1.0 eV. The authors argued that the dielectric screening effect is underestimated within the random-phase approximation, thus overestimating the self-energy correction in the subsequent *GW* calculations. In addition, lattice polarization contributions to the dielectric screening may also play an important role. When these factors are reasonably estimated, satisfactory results can be obtained. We believe these are definitely important issues that deserve future systematic investigations.

Despite the ongoing discussion/debates on the accuracy of the *GW* calculations for these systems, the two issues that we have discussed in this work are well recognized. First, being a (non-self-consistent) many-body perturbation theory, results calculated using the G^0W^0 method will inevitably depend on the starting zeroth-order mean-field solution. In the cases of ZnO, CuCl, and related systems, it has been shown that the G^0W^0/LDA + U approach gives significantly improved results compared with the G^0W^0/LDA approach. Even for systems in which the 3*d* are (nominally) unoccupied, the deficiency of the LDA functional will still have strong effects on the *GW* results, and the LDA + U solution serves as a better starting point for subsequent *GW* calculations. Second, the convergence of *GW* calculations should be carefully checked, particularly for complex/large systems or systems involving localized electrons. We believe that it is important to have an orthonormal and complete one-particle basis set against which the convergence of the *GW* results can be tested. Plane-wave-based methods have the advantage of naturally having an orthonormal complete basis set, facilitating systematic convergence tests (although the computational cost may be prohibitively expensive using the conventional *GW* approach). Our recently developed method [55] allows fully converged *GW* calculations at a fractional of computational cost compared with the conventional approach, alleviating a major computational difficulty of *GW* calculations for large/complex systems and systems involving localized states.

IV. SUMMARY

Accurate calculations of the quasiparticle properties of transition-metal oxides remain a major challenge. However, it is rather unexpected that even for some simple oxides, i.e., oxides that are not normally considered strongly correlated, theory seems to have difficulties in predicting some of the most basic but important properties such as the quasiparticle band gap. Not only were previous G^0W^0 calculations not able to reproduce experimental results for $SrTiO_3$ and $BaTiO_3$, there is also a large spread among theoretical results. In this work we show that both issues can be resolved if the G^0W^0 calculations are carried out on top of the LDA + U solutions and are properly converged. Depending on truncation parameters used, our G^0W^0/LDA calculations give an indirect band gap ranging from 3.47 to 3.82 eV for $SrTiO_3$. Fully converged G^0W^0/LDA calculations predict an indirect gap of 3.75 eV for $SrTiO_3$ and 3.62 eV for $BaTiO_3$. These results are consistent with published results calculated at the same level of theory. Using a moderate U ($U^{\text{eff}} = 4.0$ eV), our G^0W^0/LDA + U calculations give an indirect gap of 3.38 eV for $SrTiO_3$ and 3.23 eV for $BaTiO_3$, to be compared with the experimental values of 3.25 and 3.15 eV, respectively. The use of the LDA + U solution, as opposed to the LDA one, as a starting point for subsequent *GW* calculations is justified since it is now well understood that local or semilocal energy functionals are not able to describe well the localized 3*d* states, even though the 3*d* states are nominally unoccupied in these systems. Our calculations also take advantage of a recently developed accelerated method. Using this method we can afford to effectively include all conduction bands (allowed by the Hilbert space of the Kohn-Sham Hamiltonian of the system) in *GW* calculations at a fraction of the computational cost compared with the conventional approach.

ACKNOWLEDGMENTS

This work is supported by the National Science Foundation under Grants No. DMR-1506669 and No. DMREF-1626967. Work at SHU is supported by the National Natural Science Foundation of China (Grant No. 11929401). We acknowledge computational support from the Center for Computational Research, University at Buffalo, SUNY.

[1] L. Hedin, Phys. Rev. **139**, A796 (1965).
[2] G. Strinati, H. J. Mattausch, and W. Hanke, Phys. Rev. B **25**, 2867 (1982).
[3] M. S. Hybertsen and S. G. Louie, Phys. Rev. B **34**, 5390 (1986).
[4] R. W. Godby, M. Schlüter, and L. J. Sham, Phys. Rev. B **37**, 10159 (1988).
[5] W. Kohn and L. J. Sham, Phys. Rev. **140**, A1133 (1965).
[6] D. M. Ceperley and B. J. Alder, Phys. Rev. Lett. **45**, 566 (1980).
[7] J. P. Perdew and A. Zunger, Phys. Rev. B **23**, 5048 (1981).
[8] J. P. Perdew and Y. Wang, Phys. Rev. B **33**, 8800 (1986).
[9] J. P. Perdew, K. Burke, and M. Ernzerhof, Phys. Rev. Lett. **77**, 3865 (1996).
[10] K. Domen, S. Naito, M. Soma, T. Onishi, and K. Tamaru, J. Chem. Soc. Chem. Commun., 543 (1980).
[11] K. Iwashina and A. Kudo, J. Am. Chem. Soc. **133**, 13272 (2011).

[12] S. Suzuki, H. Matsumoto, A. Iwase, and A. Kudo, Chem. Commun. **54**, 10606 (2018).

[13] H. Lyu, T. Hisatomi, Y. Goto, M. Yoshida, T. Higashi, M. Katayama, T. Takata, T. Minegishi, H. Nishiyama, T. Yamada, Y. Sakata, K. Asakura, and K. Domen, Chem. Sci. **10**, 3196 (2019).

[14] S. Singh, P. Singh, M. Viviani, and S. Presto, Int. J. Hydrogen Energy **43**, 19242 (2018).

[15] B. L. Phoon, C. W. Lai, J. C. Juan, P.-L. Show, and W.-H. Chen, Int. J. Energy Res. **43**, 5151 (2019).

[16] A. Ohtomo and H. Y. Hwang, Nature (London) **427**, 423 (2004).

[17] N. Reyren, S. Thiel, A. D. Caviglia, L. F. Kourkoutis, G. Hammerl, C. Richter, C. W. Schneider, T. Kopp, A.-S. Rüetschi, D. Jaccard, M. Gabay, D. A. Muller, J.-M. Triscone, and J. Mannhart, Science **317**, 1196 (2007).

[18] A. Brinkman, M. Huijben, M. van Zalk, J. Huijben, U. Zeitler, J. C. Maan, W. G. van der Wiel, G. Rijnders, D. H. A. Blank, and H. Hilgenkamp, Nat. Mater. **6**, 493 (2007).

[19] J. Mannhart and D. G. Schlom, Science **327**, 1607 (2010).

[20] M. Lorenz, M. S. R. Rao, T. Venkatesan, E. Fortunato, P. Barquinha, R. Branquinho, D. Salgueiro, R. Martins, E. Carlos, A. Liu, F. K. Shan, M. Grundmann, H. Boschker, J. Mukherjee, M. Priyadarshini, N. DasGupta, D. J. Rogers, F. H. Teherani, E. V. Sandana, P. Bove *et al.*, J. Phys. D **49**, 433001 (2016).

[21] K. A. Müller and H. Burkard, Phys. Rev. B **19**, 3593 (1979).

[22] A. G. Chynoweth, Phys. Rev. **102**, 705 (1956).

[23] W. Koch, R. Munser, W. Ruppel, and P. Würfel, Solid State Commun. **17**, 847 (1975).

[24] W. T. H. Koch, R. Munser, W. Ruppel, and P. Würfel, Ferroelectrics **13**, 305 (1976).

[25] S. M. Young and A. M. Rappe, Phys. Rev. Lett. **109**, 116601 (2012).

[26] O. Saburi, J. Phys. Soc. Jpn. **14**, 1159 (1959).

[27] Y. L. Chen and S. F. Yang, Adv. Appl. Ceram. **110**, 257 (2011).

[28] M. Cardona, Phys. Rev. **140**, A651 (1965).

[29] D. Bäuerle, W. Braun, V. Saile, G. Sprüssel, and E. E. Koch, Z. Phys. B **29**, 179 (1978).

[30] K. van Benthem, C. Elsässer, and R. H. French, J. Appl. Phys. **90**, 6156 (2001).

[31] D. J. Kok, K. Irmscher, M. Naumann, C. Guguschev, Z. Galazka, and R. Uecker, Phys. Status Solidi A **212**, 1880 (2015).

[32] P. K. Gogoi and D. Schmidt, Phys. Rev. B **93**, 075204 (2016).

[33] K. Suzuki and K. Kijima, Jpn. J. Appl. Phys. **44**, 2081 (2005).

[34] C. Friedrich, S. Blügel, and A. Schindlmayr, Phys. Rev. B **81**, 125102 (2010).

[35] R. F. Berger, C. J. Fennie, and J. B. Neaton, Phys. Rev. Lett. **107**, 146804 (2011).

[36] A. Benrekia, N. Benkhettou, A. Nassour, M. Driz, M. Sahnoun, and S. Lebégue, Phys. B: Condens. Matter **407**, 2632 (2012).

[37] L. Sponza, V. Véniard, F. Sottile, C. Giorgetti, and L. Reining, Phys. Rev. B **87**, 235102 (2013).

[38] G. Kang, Y. Kang, and S. Han, Phys. Rev. B **91**, 155141 (2015).

[39] Z. Ergönenc, B. Kim, P. Liu, G. Kresse, and C. Franchini, Phys. Rev. Mater. **2**, 024601 (2018).

[40] C. Bhandari, M. van Schilfgaarde, T. Kotani, and W. R. L. Lambrecht, Phys. Rev. Mater. **2**, 013807 (2018).

[41] S. Sanna, C. Thierfelder, S. Wippermann, T. P. Sinha, and W. G. Schmidt, Phys. Rev. B **83**, 054112 (2011).

[42] B.-C. Shih, Y. Xue, P. Zhang, M. L. Cohen, and S. G. Louie, Phys. Rev. Lett. **105**, 146401 (2010).

[43] C. Friedrich, M. C. Müller, and S. Blügel, Phys. Rev. B **83**, 081101(R) (2011).

[44] W. Gao, W. Xia, Y. Wu, W. Ren, X. Gao, and P. Zhang, Phys. Rev. B **98**, 045108 (2018).

[45] M.-Y. Zhang and H. Jiang, Phys. Rev. B **100**, 205123 (2019).

[46] V. I. Anisimov, J. Zaanen, and O. K. Andersen, Phys. Rev. B **44**, 943 (1991).

[47] V. I. Anisimov, I. V. Solovyev, M. A. Korotin, M. T. Czyżyk, and G. A. Sawatzky, Phys. Rev. B **48**, 16929 (1993).

[48] E. Kioupakis, P. Zhang, M. L. Cohen, and S. G. Louie, Phys. Rev. B **77**, 155114 (2008).

[49] H. Jiang, R. I. Gomez-Abal, P. Rinke, and M. Scheffler, Phys. Rev. B **82**, 045108 (2010).

[50] B. G. Pfrommer, J. Demmel, and H. Simon, J. Comput. Phys. **150**, 287 (1999).

[51] N. Troullier and J. L. Martins, Phys. Rev. B **43**, 1993 (1991).

[52] Y. A. Abramov, V. G. Tsirelson, V. E. Zavodnik, S. A. Ivanov, and B. I. D., Acta Crystallogr. Sect. B **51**, 942 (1995).

[53] G. H. Kwei, A. C. Lawson, S. J. L. Billinge, and S. W. Cheong, J. Phys. Chem. **97**, 2368 (1993).

[54] J. Deslippe, G. Samsonidze, D. A. Strubbe, M. Jain, M. L. Cohen, and S. G. Louie, Comput. Phys. Commun. **183**, 1269 (2012).

[55] W. Gao, W. Xia, X. Gao, and P. Zhang, Sci. Rep. **6**, 36849 (2016).

[56] P. Zhang, W. Luo, V. H. Crespi, M. L. Cohen, and S. G. Louie, Phys. Rev. B **70**, 085108 (2004).

[57] T. Miyake, P. Zhang, M. L. Cohen, and S. G. Louie, Phys. Rev. B **74**, 245213 (2006).

[58] T. Kotani, J. Phys.: Condens. Matter **12**, 2413 (2000).

[59] T. Miyake and F. Aryasetiawan, Phys. Rev. B **77**, 085122 (2008).

[60] T. Miyake, F. Aryasetiawan, and M. Imada, Phys. Rev. B **80**, 155134 (2009).

[61] B.-C. Shih, Y. Zhang, W. Zhang, and P. Zhang, Phys. Rev. B **85**, 045132 (2012).

[62] B.-C. Shih, T. A. Abtew, X. Yuan, W. Zhang, and P. Zhang, Phys. Rev. B **86**, 165124 (2012).

[63] M. Stankovski, G. Antonius, D. Waroquiers, A. Miglio, H. Dixit, K. Sankaran, M. Giantomassi, X. Gonze, M. Côté, and G.-M. Rignanese, Phys. Rev. B **84**, 241201(R) (2011).

[64] M. Usuda, N. Hamada, T. Kotani, and M. van Schilfgaarde, Phys. Rev. B **66**, 125101 (2002).

[65] M. Shishkin and G. Kresse, Phys. Rev. B **75**, 235102 (2007).

[66] M. Zhang, S. Ono, N. Nagatsuka, and K. Ohno, Phys. Rev. B **93**, 155116 (2016).